Proceedings of ICTACEM 2017
International Conference on Theoretical, Applied, Computational and Experimental Mechanics
December 28-30, 2017, IIT Kharagpur, India
ICTACEM-2017/615

Damage Detection of Laminated Composite Shells using Unified Particle Swarm Optimization

T. R. Jebieshia*, D. K. Maiti†, D. Maity‡

Abstract

Present study deals with the damage identification in laminated composite shell structures using Unified Particle Swarm Optimization (UPSO) technique. Broad application of Composite structures in various engineering field drives the need for damage analysis and structural health monitoring. As the damages in composite materials are of anisotropic in nature, the authors are interested in modeling the damage anisotropically. This damage identification process includes two phases: forward and inverse. Anisotropic damage analysis of composite shell structures is the initial step which has been carried out using Finite Element Method (FEM) and for the inverse procedure, an algorithm or optimization method is used to locate and quantify the damages in the structure. Numerical damage assessment of shell structures using UPSO as well as thorough comparative analysis with various PSO algorithms has also been carried out.

Keywords: Anisotropic damage, FEM, Laminated Composite Shells, Particle Swarm Optimization

1 Introduction

Composite Shell structures are widely being used in various engineering applications such as pressure vessels, submarines, aircraft, etc. as the composite materials have high strength to weight ratio and numerous advantages over conventional engineering materials. Even though the composite materials possess huge advantages, the are prone to various defects as well. Due to the damages, the physical properties of the structures, such as mass, stiffness and damping, etc. may change and thus affect the dynamics characteristics. Various authors [1–10] studied the static and free vibration characteristics of healthy as well as damaged shell structures. The dynamic parameters such as natural frequencies, mode shapes etc., can be used to assess the damages. Numerous vibration based damage detection researches [11–20] has been carried out for laminated composite shell structures.

2 Theoretical formulation

The governing differential equations for the present numerical analysis of shell structures have been formulated using First order Shear Deformation Theory (FSDT) [21] then implemented the problem into MATLAB environment to obtain the various results.

[a]Research Scholar, Department of Aerospace Engineering, Indian Institute of Technology Kharagpur
[b]Professor, Department of Aerospace Engineering, Indian Institute of Technology Kharagpur
[c]Professor, Department of Civil Engineering, Indian Institute of Technology Kharagpur

The elastic constitutive relationships for anisotropic damage mechanics have been implemented in the present finite element analysis. Valliappan et al. [22] developed a finite element model of anisotropic damage based on the structural stiffness reduction factor. For the present damage assessment method, Particle Swarm Optimization has been used as an algorithm for the inverse method.

2.1 Finite Element Formulation

The finite element analysis was performed using an eight-noded curved isoparametric serendipity quadratic element with five degrees of freedom (u, v, w, ϕ_x *and* ϕ_y), per node have been used to discretize the composite panels. u, v, *and* w are the displacement components in x, y *and* z-directions, and ϕ_x *and* ϕ_y are the rotations of the cross-section perpendicular to x and y axes respectively. The shape function for 8-noded isoparametric element geometry can be defined as:

$$N_i = \left\{ \begin{array}{c} (1+\zeta\zeta_i)(1+\eta\eta_i)(\zeta\zeta_i+\eta\eta_i-1)/4, \quad for\, i=1,2,3,4 \\ (1-\zeta^2)(1+\eta\eta_i)/2, \quad for\, i=5,7 \\ (1+\zeta\zeta_i)(1-\eta^2)/2, \quad for\, i=6,8 \end{array} \right\} \tag{1}$$

where, ζ and η are the local co-ordinates of the element, and ζ_i and η_i are the co-ordinates of i^{th} node.

A simple first order shear deformation theory in which transverse shear strains are assumed to be constant across the plate thickness are considered. The displacement components are assumed to be in the form:

$$\left[\begin{array}{c} u(x,y,z) \\ v(x,y,z) \\ w(x,y,z) \end{array} \right] = \left[\begin{array}{c} u_0(x,y) \\ v_0(x,y) \\ w_0(x,y) \end{array} \right] + z \left[\begin{array}{c} \phi_x(x,y) \\ \phi_y(x,y) \\ 0 \end{array} \right] \tag{2}$$

u_0, v_0, w_0 are the displacements of a point on the mid plane $(x, y, 0)$ and ϕ_x, ϕ_y are the rotations of the cross-section perpendicular to x and y axes respectively

2.2 Anisotropic Damage

As the composite materials exhibits anisotropic properties, the analysis of damages in composite structures is much more critical than that of isotropic structures. The initial scalar parameter based damage mechanics were used to measure the damage variable under the assumption of isotropic damage in the material. For complex defects and their distribution, it is essential to use tensorial descriptions of damage [23, 24]. The anisotropic damage is parametrically incorporated into the present finite element formulation by considering the principle damage parameter or variables, Γ_i which depicts reduction in effective load bearing area [23–25] and is given as:

$$\Gamma_i = \frac{A_i - A_i^*}{A_i} \tag{3}$$

where A_i and A_i^* (i = 1, 2), are the undamaged and damaged areas with unit normal n_i and n_i^* respectively, n_i is the orthotropic damage co-ordinate system.

It is assumed that the internal forces acting on any damaged section are the same as the one before damage. Therefore, $\sigma_{ij}\delta_{jk}A_k = \sigma_{ij}^*\delta_{jk}A_k^*$, where σ_{ij} and σ_{ij}^* are the components of the Cauchy stress and effective (net) stress tensor respectively, and δ_{ij} is the Kronecker tensor.

The damage model should not assume the damage tensor to be symmetric in order to define the damage effectively in composites materials. Therefore the effective non-symmetric stress tensor relation, which is the compatibility relation of the effective shear stress components can be given as: $\sigma_{21}^* = \frac{1-\Gamma_2}{1-\Gamma_1}\sigma_{12}^*$.

2.3 Governing differential equation

It is convenient to derive the equation of motion for the free vibration of the composite structure through Hamilton's principle. Considering elastic strain energy due to bending and non-mechanical forces, Hamilton's principle is expressed as: $\int \delta(T-U)dt = 0$

$$\begin{aligned} Kinetic\,Energy,\, T &= \frac{1}{2}\left\{\dot{d}\right\}^T[M]\left\{\dot{d}\right\} \\ Strain\,Energy\,due\,to\,bending,\, U &= \frac{1}{2}\left\{\{d\}\right\}^T[K]\{d\} \end{aligned}$$

For free, undamped vibrating system, the governing differential equation for dynamic equilibrium can be given as:

$$[M]\{\ddot{d}\} + [K]\{d\} = 0$$

. Or $\{[K] - \omega^2[M]\}d = 0$; ω is the natural frequency, $\{d\}$ is the displacement vector, $[M]$, $[K]$ is the mass and stiffness matrices respectively.

Elemental elastic stiffness matrix can be given as: $K_{d\,or\,ud}^{(e)} = \int_V B^{(e)^T} D_{d\,or\,ud}\; B^{(e)} dA^{(e)} dz$

Elemental Mass Matrix can be given as: $[M]^e = \int_v [N]^T[\rho][N]\,dA\,dz$

where $[N]$ *is the shape function matrix, and* $[\rho] = \rho \begin{bmatrix} 1 & 0 & 0 & z & 0 \\ 0 & 1 & 0 & 0 & z \\ 0 & 0 & 1 & 0 & 0 \\ z & 0 & 0 & z^2 & 0 \\ 0 & z & 0 & 0 & z^2 \end{bmatrix}$, ρ is the density of the material.

2.4 Optimization Technique

For the present damage detection studies, Particle Swarm Optimization (PSO), a population based algorithm has been considered. PSO is first proposed by Kennedy and Eberhart [26] inspired by the collective motion of insects and birds trying to reach an unknown destination,

known as "swarm behavior". This process involves both social interaction and intelligence so that birds, insects, fish, etc., learn from their own experience (self experience) and also from the experience of others around them (social experience) [27]. PSO algorithm has advantages lies in its simplicity and architecture (requires updating of two simple equations) and fast rate of convergence to an optimal solution. In spite of these advantages, the main drawback associated with standard PSO is that the algorithm may be trapped into some local optima. This may cause the prediction of wrong results. Further, to improve its efficiency, numerous alternations and variations are proposed to the standard PSO algorithm.

2.4.1 Simplified Particle Swarm Optimization (SPSO)

The two simplified equation to update the velocity and position of the particles for the Simplified PSO algorithm is given as:

$$v(t+1) = v(t) + c_1 r_1 (P_l - x(t)) + c_2 r_2 (P_g - x(t)) \tag{4a}$$

$$x(t+1) = x(t) + v(t+1) \tag{4b}$$

where, P_l is the local best position and P_g is the global best position. The parameters c_1 and c_2 are called acceleration coefficients which influence the maximum size of the step that a particle can take in a single iteration. In the SPSO method the accelerations coefficients are kept constant, $c_1 = c_2 = 2.$, r terms denote random numbers between [0, 1].

2.4.2 Improved Particle Swarm Optimization (IPSO)

The above method is not accurate due to the absence of inertia weight (which governs how much of the previous velocity should be retained from the previous time) in the velocity equation. The inertia weight parameter w, has been added in SPSO to improve the efficiency of the algorithm. $w = w_{max} - \left(\frac{(w_{max} - w_{min})}{t_{max}} * t\right)$. In the Improved PSO, the acceleration coefficients (cognitive and social coefficients) are non-linear in nature. Therefore, improved balance between global and local search abilities can be attained. The large cognitive component may increase the global search capability to avoid trapping into local optima, as well as the large social component enhances the local search capability. In the IPSO, the consideration is taken as: $c_1 + c_2 = 3$.

$$v(t+1) = w * v(t) + c_1 r_1 (P_i - x(t)) + c_2 r_2 (P_g - x(t)) \tag{5a}$$

$$x(t+1) = x(t) + v(t+1) \tag{5b}$$

where, $c_1 = 2.5 + 2 * \left(\frac{iter}{max.iter}\right)^2 - \frac{4iter}{max.iter}$, $c_2 = 3 - c_1$, r terms denote random numbers between [0, 1] and $w = w_{max} - \left(\frac{(w_{max} - w_{min})iter}{max.iter}\right)$; w_{max} =0.9, $w_{min} = 0.4$

2.4.3 Unified Particle Swarm Optimization (UPSO)

Unified Particle Swarm Optimization (UPSO) is one of the PSO algorithm that has the ability to harness both exploration and exploitation capacity simultaneously [28] by balancing the influence of both global and local search directions simultaneously. Mathematically, for a swarm size of P number of particles, in an S - dimensional search space, each particle occupies a position $X_i = \{x_{i1}, x_{i2}, ..., x_{id}, ..., x_{iS}\}$, with a velocity $V_i = \{v_{i1}, v_{i2}, ..., v_{id}, ..., v_{iS}\}$, where $i = 1, 2, .., P$ and $d = 1, 2, ..., S$. In each iteration, each particle moves towards its best position and the best particle *pbest* in the swarm. The change of position of each particle can be computed according to the distance between the current position and its previous best position and the distance between the current position and the best position of swarm. Suppose the best previously visited position of the i^{th} particle gives the best fitness value as $Pbest = \{pbest_{i1}, pbest_{i2}, ..., pbest_{id}, ..., pbest_{iS}\}$ and the best previously visited position of the swarm gives best fitness as $Gbest = \{gbest_1, gbest_2, ..., gbest_d, ..., gbest_S\}$. The best position so far found by any of its neighborhood is $lbest = \{lbest_{i1}, lbest_{i2}, ..., lbest_{id}, ..., lbest_{iS}\}$. Let G_{ij}^{t+1} and L_{ij}^{t+1} denotes the velocity update of i^{th} particle in global and local variants of PSO respectively for the $(t+1)^{th}$ iteration in the d^{th} dimensional search space as given by,

$$G_{id}^{t+1} = \chi \left[v_{id}^{t} + c_1 r_1 \left(pbest_{id} - x_{id}^{t} \right) + c_2 r_2 \left(gbest_d - x_{id}^{t} \right) \right] \tag{6a}$$

$$L_{id}^{t+1} = \chi \left[v_{id}^{t} + c_1 r_3 \left(pbest_{id} - x_{id}^{t} \right) + c_2 r_4 \left(lbest_{id} - x_{id}^{t} \right) \right] \tag{6b}$$

χ denotes the constriction factor which equals to 0.72984. c_1 and c_2 are two acceleration coefficients and is considered as 2.05 each in present study. Finally, all r terms denote random numbers between [0, 1] and independent of each other. Combining Equations (6a) and (6b), the aggregate updating velocity of the particles in the search directions is defined as,

$$V_{id}^{t+1} = uG_{id}^{t+1} + (1-u)L_{id}^{t+1}, \;\; u \,\varepsilon\, [0, 1] \tag{7}$$

The new position of the particles for $(t+1)^{th}$ iteration is, $x_{id}^{t+1} = x_{id}^{t} + V_{id}^{t+1}, \;\; \forall\, i \,\varepsilon\, P \; and \; \forall\, d \,\varepsilon\, S$

The parameter u in Equation 7 is called the unification factor and its value is modified throughout the iteration according to the equation,

$$u(t) = exp\left(\frac{t\, log(2.0)}{t_{max}} \right) - 1.0 \tag{8}$$

where t_{max} is the maximum number of iteration.

2.5 Objective Function

Objective function is an equation to be optimized given certain constraints and with variables that need to be minimized or maximized. For the present damage assessment study, combination of both natural frequency and mode shape is used as the objective function [13]. The free vibration and damage analysis of laminated composite plate is done using Finite Element Method (FEM). An eight-noded serendipity quadratic element have been used to discretize the

plate structure.

Natural frequencies and mode shapes obtained from the damaged structure are used for constructing the objective function [29] of the present problem and is given as:

$$F = \sqrt{\frac{1}{n}\sum_{i=1}^{n}\left(\left(\frac{f_i^m}{f_i^c}\right)-1\right)^2} + \sum_{i=1}^{n}(1-MAC_{ii}) \tag{9}$$

where Modal Assurance Criterion, $MAC_{ii} = \frac{(\phi_{m,i}^T \phi_{c,i})^2}{(\phi_{m,i}^T \phi_{m,i})(\phi_{c,i}^T \phi_{c,i})}$

The terms f_i^m are the measured natural frequencies for damaged structure and f_i^c are the natural frequency computed from numerical analysis (finite element simulation) for damaged structure. n is the number of input response parameters.

3 Results and Discussion

Finite element formulation (Sec. 2.1) has been developed in Matlab environment to obtain the vibration response. To validate the efficacy of the present formulation for composite shells, the results (first few natural frequencies) obtained for different composite shell structures are compared with that of the available literature.

3.1 Validation of the present finite element formulation

For the validation purpose, first few natural frequencies of cantilevered cylindrical shell ($E_1 = 128\,GPa$, $E_2 = 11\,GPa$, $G_{12} = 4.48\,GPa$, $G_{13} = 1.53\,GPa$, $\nu = 0.25$, h/ply = 0.13 mm, $a = 15.24\,cm$, $b = 7.62\,cm$, $\rho = 1500\,\mathrm{kg/m^3}$, $R_x = \infty$, $R_y = 12.75\,cm$, $R_{xy} = \infty$) is compared with the numerical and experimental results by Crawley [30] and is tabulated in Table 1.

The fundamental natural frequency of a square laminated twisted composite cantilever plate ($E_1 = 141\,GPa$, $E_2 = 9.23\,GPa$, $G_{12} = 5.95\,GPa$, $G_{23} = 2.96\,GPa$, $\nu_{12} = 0.313$, h = 2mm, a = b = 500mm, $\rho = 1580\,\mathrm{kg/m^3}$, $R_x = \infty$, $R_y = \infty$) with different ply orientations is considered for the comparative study and is shown in Table 2

Non-dimensional free vibration frequencies for first four modes of singly curved cantilever panels ($E_1 = 141GPa$, $E_2 = 9.23GPa$, $G_{12} = 5.95GPa$, $G_{23} = 2.96GPa$, $\nu_{12} = 0.313$, a = b = 500 mm, h = 2 mm, $\rho = 1500\,\mathrm{kg/m^3}$, $R_x = \infty$, $b/R_y = 0.25$, $R_{xy} = \infty$) obtained using present finite element program are compared with that of the available literature and are tabulated in Table 3. From the Table 1, 2 and 3, it is clear that the results from the present finite element formulation is well matching with that of the available literature.

Table 1: Natural frequencies in Hz of cantilevered cylindrical shell

Present FEM	Experimental Results [30]	Calculated Results [30]
$[0_2/\pm 30]_s$		
166.55	161	165.7
282.76	254.1	289.6
606.23	555.6	597.1
709.91	670	718.5
828.52	794	833.3
[0/45/-45/90]s		
196.49	177.0	192.4
229.51	201.8	236.1
720.84	645.0	705.8
805.91	754.0	808.2
980.85	884.0	980.6
[45/-45/-45/45]s		
140.51	145.3	147
236.03	222.0	238
758.07	712.0	768.1
777.64	774.2	812.1
1041.45	997.0	1036

Table 2: Non-dimensional fundamental natural frequencies of twisted plates with different ply orientations

Angle of twist	Ply orientation	Present FEM	[31]
0	0/90	0.4829	0.4829
	0/90/0/90	0.6872	0.6872
	0/90/90/0	0.9565	0.9565
	0/90/0/90/0/90/0/90	0.7294	0.7294
10	0/90	0.4805	0.4800
	0/90/0/90	0.6835	0.6831
	0/90/90/0	0.9510	0.9508
	0/90/0/90/0/90/0/90	0.7254	0.7251
20	0/90	0.4731	0.4708
	0/90/0/90	0.6717	0.6700
	0/90/90/0	0.9337	0.9326
	0/90/0/90/0/90/0/90	0.7127	0.7112
30	0/90	0.4597	0.4540
	0/90/0/90	0.6501	0.6461
	0/90/90/0	0.9021	0.8993
	0/90/0/90/0/90/0/90	0.6896	0.6858

Table 3: Natural frequencies of singly curved cantilever panel

Ply orientation		Non-dimensional frequencies			
		Mode 1	Mode 2	Mode 3	Mode 4
0/0/0	Present	2.119	2.361	5.259	5.5697
	[31]	2.112	2.349	5.250	5.532
90/90/90	Present	1.037	1.921	4.180	6.308
	[31]	1.034	1.918	4.164	6.268

3.2 Damage Detection

For the damage assessment, composite shell with damage having material properties and dimension, tabulates in Table 4 are considered. These composite shells of various ply orientations has been discretized into ten elements as shown in Figure 1. Tables 5 and 8 shows the changes in natural frequencies for various damages cases. Damage assessment results for single and multiple damage locations are given in Tables 6, 7 and 9. From Tables 6, 7 and 9, it is clear that UPSO algorithm gives the accurate results as compared to other PSO techniques.

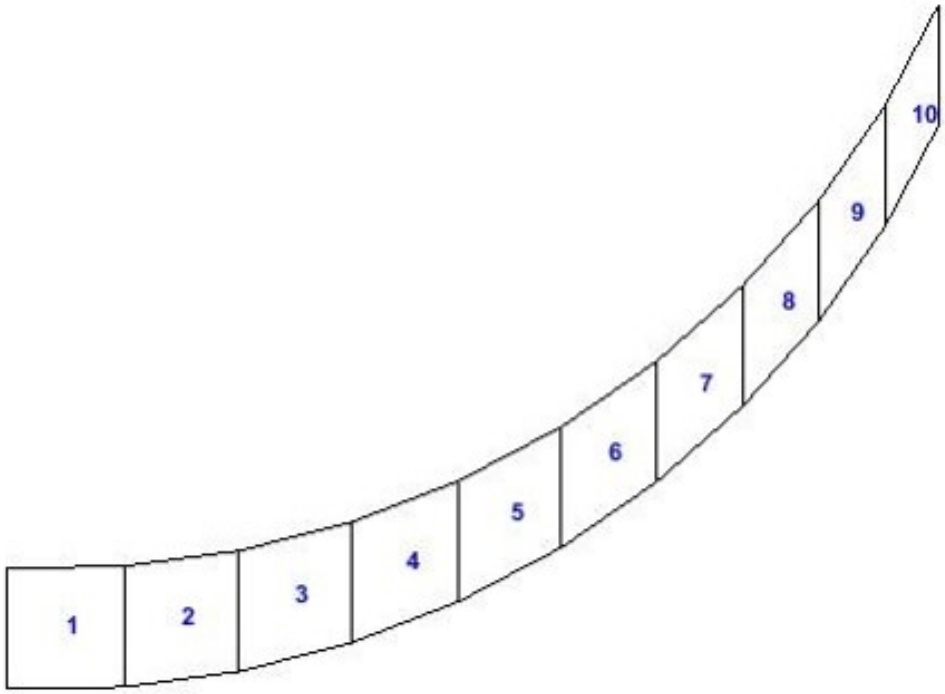

Figure 1: Finite Element discretization of singly curved shell

Table 4: Material properties of shell considered for damage assessment

Material/Geometric property	Material Model 1 (MM1)	Material Model 2 (MM2)
Elastic modulus,E_{11}	134 GPa	128 GPa
Elastic modulus, E_{22}	10.3 GPa	11 GPa
Shear modulus, $G_{12} = G_{13}$	5 GPa	4.48 GPa
Shear modulus, G_{23}	2.96 GPa	2.84 GPa
Poison's Ratio, ν_{12}	0.33	0.25
Density of the material, ρ	1480 kg/m^3	1500 kg/m^3
Length, l	127 mm	152.4 mm
Breadth, b	12.7 mm	76.2 mm
Total thickness, t	10.16 mm	1.04 mm
Radius of curvature, R_y	50.8 mm	127.5 mm
Ply orientation	$(0/90/0/90)_s$	$[(45/-45)_s]_2$

Table 5: Frequency change for MM1

Change in Natural Frequency (Hz)		
Undamaged	Single Element Damaged	Two Element Damage
779.12	790.17	772.69
865.34	864.90	854.81
2937.11	3215.89	3230.55
3900.09	4164.91	4137.21
4687.95	4684.48	4655.19
8816.00	9660.30	9556.90

Table 6: Single element damage case

Algorithm	Damaged Layer	Damaged Element	Damage Parameter	
			Γ_1	Γ_2
Actual	7	5	0.4	0.25
UPSO	7	5	0.4	0.25
PSO	7	5	0.414	0.22
IPSO	7	5	0.404	0.242

Table 7: Two element damage case

Algorithm	Damaged Layer	Damaged Element	Damage Parameter	
			Γ_1	Γ_2
Actual	1	3	0.3	0.1
	5	8	0.45	0.2
UPSO	1	3	0.3	0.21
	5	8	0.45	0.2
PSO	1	3	0.3054	0.0674
	5	8	0.4305	0
IPSO	1	3	0.2768	0.3617
	1	7	0	0

Table 8: Change in natural frequency for (MM2)

Natural Frequency in Hz	
Undamaged	Damage
147.2859	146.6426
463.5675	458.3315
858.6222	858.7514
1355.1450	1331.1368
1756.3656	1738.3494
2003.4470	1966.3235

Table 9: Three element damage case

Algorithm	Damaged Layer	Damaged Element	Damage Parameter	
			Γ_1	Γ_2
Actual	1	3	0.3	0.1
	4	7	0.45	0.2
	7	10	0.5	0.3
UPSO	1	3	0.3	0.1
	4	7	0.45	0.2
	7	10	0.5	0.3
PSO	1	3	0.0	0.155
	4	7	0.298	0.431
	7	10	0.407	0.5
IPSO	3	3	0.2603	0.328
	6	7	0.2914	0.3448
	7	10	0.4064	0.4988

4 Conclusion

A numerical procedure is presented to detect and quantify the damages in a composite shell structures based on changes in natural frequency and mode shape data using UPSO technique. The proposed methodology is demonstrated using a numerically simulated composite structures containing single and multiple damages. Thorough comparative study has been carried out with other PSO algorithms to prove the efficiency of present UPSO technique. As indicated by the simulation results, the present method is able to detect and quantify the damage accurately using first few natural frequencies and corresponding mode shapes for considered damage cases.

References

[1] AW Leissa, J K Lee, and A J Wang. Vibrations of cantilevered shallow cylindrical shells of rectangular planform. *Journal of Sound and Vibrationibration*, 78(3):311–328, 1981.

[2] Mohamad S. Qatu and Arthur W. Leissa. Free Vibrations of Completely Free Doubly Curved Laminated Composite Shallow Shells. *Journal of Sound and Vibration*, 151(1):9–29, 1991.

[3] Robin S. Langley. A Dynamic Vibration Stiffness Technique for the Analysis of Stiffened Shell Structures. *Journal of Sound and Vibration*, 156(3):521–540, 1992.

[4] P.K. Parhi, S.K. Bhattacharyya, and P.K. Sinha. Hygrothermal Effects on the Dynamic Behavior of Multiple Delaminated Composite Plates and Shells. *Journal of Sound and Vibration*, 248(2):195–214, 2001.

[5] W H Lee and S C Han. Free and forced vibration analysis of laminated composite plates and shells using a 9-node assumed strain shell element. *Computational Mechanics*, 39(1):41–58, 2006.

[6] Amit Karmakar and Kikuo Kishimoto. Free vibration analysis of delaminated composite pretwisted rotating shells-a finite element approach. *JSME International Journal Series A*, 49(4):492–502, 2006.

[7] W. Wagner and C. Balzani. Simulation of delamination in stringer stiffened fiber-reinforced composite shells. *Computers and Structures*, 86(9):930–939, 2008.

[8] Gz Voyiadjis and P Woelke. *Elasto-plastic and damage analysis of plates and shells*. Springer, New York, 2008.

[9] M. Biswal, S.K. Sahu, and A.V. Asha. Experimental and numerical studies on free vibration of laminated composite shallow shells in hygrothermal environment. *Composite Structures*, 127:165–174, 2015.

[10] Kun Xie, Meixia Chen, and Zuhui Li. An analytic method for free and forced vibration analysis of stepped conical shells with arbitrary boundary conditions. *Thin-Walled Structures*, 111(November 2016):126–137, 2017.

[11] Herve Abdi. Structural Damage Detection and Identification Using Neural Networks. *AIAA Journal*, 32(1):176–183, 1994.

[12] Kim Ho Ip and Ping Cheung Tse. Locating damage in circular cylindrical composite shells based on frequency sensitivities and mode shapes. *European Journal of Mechanics, A/Solids*, 21(4):615–628, 2002.

[13] Usik Lee and Sunghwan Kim. Identification of multiple directional damages in a thin cylindrical shell. *International Journal of Solids and Structures*, 43(9):2723–2743, may 2006.

[14] L. Yu, L. Cheng, L. H. Yam, Y. J. Yan, and J. S. Jiang. Online damage detection for laminated composite shells partially filled with fluid. *Composite Structures*, 80(3):334–342, 2007.

[15] Huiwen Hu, Chengbo Wu, and Wei Jun Lu. Damage detection of circular hollow cylinder using modal strain energy and scanning damage index methods. *Computers and Structures*, 89(1-2):149–160, 2011.

[16] Jiawei Xiang, Toshiro Matsumoto, Yanxue Wang, and Zhansi Jiang. Detect damages in conical shells using curvature mode shape and wavelet finite element method. *International Journal of Mechanical Sciences*, 66:83–93, 2013.

[17] Ricardo de Medeiros, Marcelo Leite Ribeiro, and Volnei Tita. Computational methodology of damage detection on composite cylinders : structural health monitoring for automotive components. *International Journal of Automotive Composites*, 1(1):112–128, 2014.

[18] Yao Zhang, Seng Tjhen Lie, Zhihai Xiang, and Qiuhai Lu. A frequency shift curve based damage detection method for cylindrical shell structures. *Journal of Sound and Vibration*, 333(6):1671–1683, 2014.

[19] Ricardo de Medeiros, Murilo Sartorato, Dirk Vandepitte, and Volnei Tita. A comparative assessment of different frequency based damage detection in unidirectional composite plates using MFC sensors. *Journal of Sound and Vibration*, 383:171–190, 2016.

[20] Masoud Pedram, Akbar Esfandiari, and Mohammad Reza Khedmati. Frequency domain damage detection of plate and shell structures by finite element model updating. *Inverse Problems in Science and Engineering*, 5977(April):1–33, 2017.

[21] J.N. Reddy. *Mechanics-of-Laminated-Composite-Plates-and-Shells*. CRC Press, Texas, 2nd ed edition, 1997.

[22] S. Valliappan, V. Murti, and Z. Wohua. Finite element analysis damage mechanics of anisotropic problems. *Engineering Fracture Mechanics*, 35(6):1061–1071, 1990.

[23] Jean Lemaitre. How to use damage mechanics. *Nuclear Engineering and Design*, 80:233–245, 1984.

[24] Jean Lemaitre and Jacques Dufailly. Damage measurements. *Engineering Fracture Mechanics*, 28(516):643–661, 1987.

[25] Jean Lemaitre. Coupled Elasto-Plasticity and Damage Constitutive Equations. *Computer Methods in Applied Mechanics and Engineering*, 51:31–49, 1985.

[26] J Kennedy and R Eberhart. Particle swarm optimization. *Neural Networks, 1995. Proceedings., IEEE International Conference on*, 4:1942–1948 vol.4, 1995.

[27] S.C. Mohan, D.K. Maiti, and D. Maity. Structural damage assessment using FRF employing particle swarm optimization. *Applied Mathematics and Computation*, 219(20):10387–10400, jun 2013.

[28] K E Parsopoulos and M N Vrahatis. Unified Particle Swarm Optimization for Solving Constrained Engineering Optimization Problems. *Advances in natural computation, Springer*, 3612:582–591, 2005.

[29] Bharadwaj Nanda, Damodar Maity, and Dipak K. Maiti. Modal parameter based inverse approach for structural joint damage assessment using unified particle swarm optimization. *Applied Mathematics and Computation*, 242:407–422, 2014.

[30] E. F. Crawley. The Natural Modes of Graphite/Epoxy Cantilever Plates and Shells. *Journal of Composite Materials*, 13(3):195–205, 1979.

[31] A.V. Asha. Parametric Resonance Characteristics of Laminated Composite Twisted Cantilever Panels. *PhD thesis*, (April), 2008.